FACTORS AFFECTING THE EXPANSION AND CRACKING OF MODEL BRIDGE PILES IN SEAWATER, AND THE EFFECTS OF MECHANICAL CONFINEMENT

Ahmad Shayan*, Aimin Xu and Roger Olasiman

ARRB Group Ltd, 500 Burwood Highway, VERMONT SOUTH, VIC 3133, Australia

Abstract

Deterioration of some Australian bridge piles, submerged in seawater, has been attributed mainly to AAR and DEF. Sixteen model piles were manufactured at 20°C (ambient) or 85°C (steam-curing), incorporating different aggregate types and cement sulfate contents, to clarify their influences on expansion under different exposure conditions.

All piles containing reactive aggregate expanded significantly, being larger in the submerged portion of piles than in the dry portion. Higher cement sulfate content exacerbated the AAR expansion, due to DEF, only in the steam-cured piles. AAR was the only cause of expansion in ambient-cured piles.

With non-reactive aggregate, DEF occurred rarely, only when high levels of temperature, alkali and sulfate were simultaneously present.

Four cracked piles were repaired through confinement by CFRP wrapping, or reinforced concrete jacketing. Extensive expansion results suggest that the confinement is only partially effective in reducing the expansion, which is continuing at lower but still deleterious levels.

Keywords: AAR, DEF, Expansion, "CFRP-wrapping", "Concrete-jacketing"

1 INTRODUCTION

Recently several serious cases of deterioration of precast piles have been noted in bridges in tidal water as well as fresh water. In some cases the concrete piles had lost a portion of the concrete and the reinforcement which caused serious concern over the load capacity of the structure concerned [1]. The causes of the deterioration appeared to be multiple and can be attributed to alkali-aggregate reaction (AAR), corrosion of steel reinforcement, internal sulfate attack (delayed ettringite formation - DEF) and salt attack from the environment. The volumetric changes in concrete, induced by AAR and DEF, cause cracking of concrete and generate stresses in the reinforcement which could exceed its yield strength. It is very important to identify the primary causes of the deterioration, because secondary causes, such as salt attack on concrete and steel reinforcement would be minimised if the concrete is free of AAR and DEF.

AAR is a well known cause of serious cracking in some affected concrete in Australia [2]. This exposes the interior of the concrete to attack by aggressive agents such as oxygen, carbon dioxide, moisture and salt water. Subsequent to AAR damage, salt ingress and corrosion of reinforcement can proceed faster causing combined deterioration [3]. Therefore, such problems could be minimised if the concrete is free from AAR, which can be achieved by correct selection of the aggregate.

Delayed ettringite formation (DEF) is related to cement composition and heat-curing temperature, applied to precast elements, as well as the exposure conditions [4]. A considerable volume of literature has been produced in this area in the past three decades, some of which is controversial [5, 6]. In Australia, no field case of DEF alone has yet been identified, and symptoms of DEF have always been associated with AAR damage. However, in an extensive laboratory experimental program [7], deleterious expansion was noted in steam cured concrete (80°C) containing non-reactive aggregate, only when high aluminate, high sulfate and high alkali contents were simultaneously present in the concrete. These conditions are often not met using currently manufactured Australian cements.

Prevention of DEF damage is different from that of AAR damage, and involves control of cement composition, such as sulfate, aluminate and alkali contents. Uninformed repair of damaged elements subjected to on-going expansion (such as AAR, DEF or corrosion) could be a waste of money. Unfortunately, the effectiveness of repair systems such as carbon-fibre reinforced polymer (CFRP) wrapping and reinforced concrete (RC) jacketing has not been adequately documented for such deteriorating concrete. Wrapping AAR-affected concrete cylinders with CFRP [8] was partially effective in reducing the expansion, but did not eliminate it. Obviously, there is a great need to develop knowledge in this area.

* Corresponding author : ahmad.shayan@arrb.com.au

This paper presents data on the factors influencing the AAR and DEF mechanisms in model piles and their relative importance in the deterioration. It also evaluates the efficiency of the two repair methods mentioned above in reducing the rate of deterioration to acceptable, non-deleterious levels.

2 EXPERIMENTAL WORK

Model piles were used in this study, details of which are given below. The factors investigated to identify the main cause(s) of deterioration of the bridge piles are presented in Table 1 and Figures (1a & 1b), where highly reactive, slowly reactive and non-reactive aggregates are designated (Hr), (Lr) and (Nr), respectively. Salt water refers to 3.5% NaCl solution. The GP cement used contained 0.58% alkali content (Na_2Oequivalent) and about 5% C_3A. The concrete mix selected contained 450 kg cement /m^3 with an elevated cement alkali level of 1.4 %, i.e., a total concrete alkali content of 6.3 kg/m^3. The water to cement ratio was 0.42, and the coarse aggregate content was 1130, 1060 and 1100 kg/m^3 for the Nr, Lr and Hr aggregates, respectively. The fine aggregate content was 690 kg/m^3 for all mixes.

Normal temperature curing is expected to generate AAR expansion alone for reactive aggregates, whereas 85 °C curing could generate both AAR and DEF with reactive aggregate, and DEF alone with non-reactive aggregate. Salt water exposure was not intended to study steel corrosion but to clarify its effects on expansion.

The objectives of the research were firstly to generate cracking in some piles, and determine the extent of the associated strain development in the concrete and the reinforcement bars. Figures (1a & 1b) show the combinations of the variables for stage 1. Secondly, it aimed at repairing some cracked piles by CFRP wrapping and concrete jacketing, and comparing their effects on restraining the expansion. Four cracked piles containing the reactive aggregate (Hr) were selected for repair in stage 2 (see later).

The specimens were labelled in the order of the aggregate type used (Nr, Lr or Hr), curing condition (N or S) and the environmental exposure (W or C). Thus, 'Hr-S-C' indicates highly reactive aggregate, steam cured pile, and half-immersion in salt water.

2.1 Specimen configuration

The cross section and elevation of the 1100 mm long model piles are shown in Figure 2. The positions of the various strain gauges are also shown. Table 2 lists the various types of strain gauges used, and Table 3 describes the locations of the various gauges.

2.2 Early age treatment and storage environment

When casting the piles, accompanying concrete cylinders (100 mm x 200 mm long) and concrete prisms (75 x 75 x 285 mm) were also made for strength testing and expansion measurement, respectively.

For the steam-cured specimens, the preheating period after casting was 2.5 -3.0 hours, after which they were placed in the steam chamber and the temperature was raised by 10 °C/ hr until it reached 85 °C. The soaking period at the maximum temperature was five hours for the first set of model piles, but 10 hours for the second set. After the steam curing period, the heating was automatically cut off and samples allowed to cool down to ambient temperature in the closed chamber.

After demoulding, all the piles were wrapped in moist cloth and, after one week, surface strain gauges were installed in appropriate locations. Subsequently, the piles were wrapped in moist cloth again and then half-immersed in their containers, either in tap water or salt solution. In the case of salt solution, the moist wrapping was present only in the top part of the pile, so that salt does not migrate up the pile. The whole assembly was then wrapped in plastic sheeting and placed at 38°C for expansion measurement. Figures 3 to 5 show the various stages of preparation of the model piles.

2.3 Expansion measurements on model piles

Strains were recorded for surface gauges and those embedded in the concrete, and on the steel bars. Almost all surface gauges failed due to breakdown of their protective coating, which resulted from moisture condensation under the humid storage environment. Reasonable readings were obtained from the other gauges, although some fibre optic gauges also failed soon after measurements started.

2.4 Repair of piles by confinement

Four cracked piles containing the reactive aggregate (Hr) were selected for repair. Piles 10 and 11 contained 2.6% SO_3 and piles 13 and 14 contained 5% SO_3 by mass of cement, all being steam cured. Piles 10 and 13 were repaired using conventional reinforced concrete jacketing, and piles 11 and 14 by the CFRP wrapping technique. Figure 6 shows the extent of cracking on the various faces of piles 11and 14.

Piles 10 and 13 were jacketed with RC and piles 11 and 14 with one layer of CFRP; the latter by the manufacturer's own technicians, and in accordance with the manufacturer's instruction. Table 5 shows details of the repair materials used in the two methods. Note that the reinforcement ratio changed from 1.4% in the original pile to 1.3% after RC jacketing.

Figure 7 illustrates a CFRP-wrapped pile, as well as the placement of steel cage and mould for RC jacketing of another pile. Note the two strain gauges to be incorporated into the RC jacket to monitor the expansion behaviour. Two foil type strain gauges were mounted on the CFRP

3 RESULTS AND DISCUSSION

3.1 Properties of concrete mixes

Figure 8 shows the results of 28-day compressive strength tests on concrete cylinders. Steam-curing somewhat reduced the 28-day strength, and the reduction was larger for the reactive than the non-reactive aggregate, indicating that steam curing probably induced some AAR expansion and micro-cracking in the concrete by the age of 28 days.

The 1-year expansion results of concrete prisms stored at 38°C, 100% RH (after the initial curing), are given in Table 4. Steam curing significantly increased the AAR expansion of concrete prism compared to normal curing, and this was more evident for the slowly reactive aggregate. The large expansion of concrete prisms containing the highly reactive aggregate (Hr) under both normal- and steam-curing conditions clearly demonstrates the high reactivity of this aggregate. Note that the AAR expansion of the reinforced piles could be less than that exhibited by the un-reinforced concrete prisms.

3.2 Strain measurements on concrete and steel gauges before repair

Results of about18 months of expansion measurement on all the piles were reported by Shayan, et al (2006) [9]. The piles containing the reactive aggregate had already developed considerable cracking by that time. The overall expansion measurements made to date, including those before and after repairing the piles are presented in the following sections.

3.3 Strain measurements on concrete gauges after repair

The repaired piles were stored again under the same conditions of 38 C, 100% RH, and strain measurements continued for all the gauges. The results presented below relate to all the measurements made on the piles to the present date, including those before and after the repair.

The expansion measurements for the concrete embedded gauges in normal- and steam-cured piles, containing the different aggregates and half-immersed in salt water, are compared in Figure 9. The piles half-immersed in water showed the same trend. To date exposure to salt water has not shown additional effects on expansion, but at later stages the reinforcement bars may show corrosion effects.

Pile expansion followed the reactivity of the aggregate in it. Steam curing increased the AAR expansion of the low-reactive aggregate, whereas the piles containing the highly reactive aggregate showed decreased expansion. The bottom portion of the pile which was immersed in water or salt solution expanded more than the top portion which was under drier condition.

The expansion trends of piles 13 and 14 (containing the Hr aggregate and 5% SO_3), and those of piles 15 and 16 (Nr aggregate and 5% SO_3) are shown in Figure 10. The two piles, with the highly reactive aggregate and additional sulfate (piles13 and 14) expanded significantly in a relatively short period. Compared to similar piles without the additional sulfate, the expansion was larger at the early ages, before the repair, indicating that DEF probably exacerbated the AAR expansion. The difference in expansion between piles with lower and higher sulfate was less significant at later ages (Figure 11).

For piles15 and 16, which incorporate the non-reactive aggregate and 5% SO_3, no AAR expansion is expected. In fact, only very small expansion was noted for pile 16, cured at ambient temperature. However, for the steam-cured pile 15, due to the high alkali and sulfate contents, and the high temperature reached within the concrete (88 °C), significant expansion and cracking was noted, which is attributed to DEF alone.

The above data show that, when the aggregate is reactive, the most prevailing damage mechanism in both the steam-cured and ambient-cured piles is the AAR. However, high sulfate contents can exacerbate the AAR expansion, through DEF, only in steam-cured piles (or large elements with high hydration temperature).

With non-reactive aggregate, DEF damage can occur only when all the contributing factors, such as high sulfate, high alkali and high curing temperature are all present simultaneously.

Based on the results of the post repair expansion measurements, it is evident that the repair has only slowed down the expansion rate, but deleterious expansion is still continuing. An option may be to install another variety of high modulus CFRP which, the manufacturer believes, may be more effective in reducing the expansion. This would need experimental verification.

The strains measured in the RC jacket and on the CFRP layer are shown in Figure 12, which indicates continuing expansion and reflects the ongoing internal expansion of the piles, as the jacket material itself is non-reactive. Neither of the methods eliminated or reduced the deleterious expansion to safe levels.

In fact, recent monitoring revealed cracking in the concrete jackets due to internal AAR expansion of the original concrete. The fact that the CFRP wrapping did not completely contain the lateral expansion could partly be attributed to the non-circular cross section of the piles. The AAR expansion induces non-uniform stresses on the side faces of the wrapped piles, which are not effectively contained by CFRP at mid-face, due to the square shape. Therefore, the side faces are free to expand. However, CRFP-wrapped cylindrical specimens used by Wigum and Thorenfeldt (2004) [8] appeared to provide more effective confinement of the AAR expansion, although still incomplete. So, the shape effect may explain the observed lack of full confinement. Based on the maximum strain measured on the CFRP (2500 μstrain) and its modulus of 240GPa, the stress generated by AAR in the CFRP is about 600MPa which is far below its tensile strength of 3800 MPa.

3.4 Strain measurements on Steel gauges

Many of the steel gauges were erratic, particularly those in steam cured concrete, and often those in the wet areas of the piles. Unrealistically high values were obtained for steel strains in the main bars of the piles with non-reactive aggregate. Those with the slowly reactive aggregate sometimes recorded very large readings and appeared to be incorrect. This is illustrated in Figures 13 for the strains measured in the main steel bars in piles with the highly reactive aggregate. The erratic behaviour of the gauges in the steam cured piles is evident. Considering that the maximum concrete expansion for piles with normal curing was around 2500 microstrains (Figure 9), the much greater steel strains measured in same piles may not be realistic.

A similar situation was observed for the steel gauges mounted on stirrups, and only strains in piles with normal curing appeared to be reasonable. The results for the piles containing the Hr aggregates are presented in Figure 14.

3.5 Comparison of fibre optic and electrical foil sensors

Results presented in Figures 15 and 16 show variability between the readings from the fibre optic gauges and the foil gauges, although the trends are similar. For the foil type, embedded concrete gauges (triangle and diamond), more expansion was recorded in the lower, wet part of the pile (1400 microstrains) than in the top part (900 microstrains). The fibre optic gauge in the wet area (**x**) appeared to have failed after one year, whereas the readings of that in the dry area (■) were similar to those of the foil gauge (diamond), indicating that the two gauges behaved similarly in the top part of the pile.

The electrical foil type of steel gauges showed higher readings than the corresponding optic fibre gauges. The bottom of pile (diamond) expanded less than the top (square) portions of piles. The fibre optic type of steel gauge in both the top and the bottom portions (triangle and x) appear to have failed after about 300 days, probably due to the wet environment.

4 CONCLUSIONS

This work was undertaken to clarify the influence of factors such as alkali-reactivity of aggregate, cement sulfate content, temperature of curing, and exposure conditions on the behaviour of bridge piles. Sixteen model pile incorporating the different factors were manufactured and their behaviours monitored by the measurement of strain both in the reinforcement steel bars and in the concrete. It has been shown that:

- The reactivity of the aggregate played the major role in the expansion and deterioration.
- Expansion was greater in the submerged wet zone of the piles.
- Steam-curing at 85 °C, per se, did not cause any deterioration in the concrete containing non-reactive aggregate, at the native SO_3 and C_3A contents of the cement.
- Steam-curing increased the reactivity of the slowly reactive (Lr) aggregate.
- Steam cured piles containing reactive aggregate expanded more than their corresponding ambient-cured piles, indicating the influence of DEF in these specimens. Probably DEF enhanced the AAR expansion. Additional sulfate increased the DEF-induced expansion.

- With non-reactive aggregate, all the other parameters (sulfate and alkali contents, and curing temperature) need to be simultaneously high for deleterious expansion to occur. This may not often be encountered in practice, whereas AAR damage can occur more often.
- Surface-mounted strain gauges were unsuitable for expansion measurement at high humidity environment used to promote AAR and DEF. Embedded concrete gauges were satisfactory. Also, steel gauges and fibre optic gauges did not perform satisfactorily in wet areas.
- Repair of damaged piles by jacketing with either CFRP or RC was only partially effective in reducing the deterioration, as expansion continued at lower but deleterious rates after repair. A higher modulus CFRP may be more effective in containing the AAR expansion. However, the square piles appear to be unsuitable for confinement by CFRP.
- It is recommended that Road Authorities lower the allowable cement sulfate content from 5% to around 3.0% - 3.5%, and limit the steam curing temperature to below 65 °C.

5 ACKNOWLEDGMENT

Three previous employees of ARRB contributed to the experimental work, namely, K. Lee, H. B. Pham and A. Hii, who were Ph.D. candidates at Monash University at the time of joining ARRB. The opinions expressed in this paper are those of the authors and do not reflect the practices or policies of the supporting organisations.

6 REFERENCES

[1] Shayan, A and Morris, H (2006): A case study: Deterioration of precast, prestressed concrete piles in marine environment. Concrete Plant & Precast Technology, BFT (Germany), Vol. 72, No. 1: 38-47.

[2] Shayan A (2003): AAR in Australia and Recent Developments. Proc. Int. Seminar on Road Construction Materials, held at the Department of Civil Engineering, Kanazawa University, Kanazawa, Japan, 28 October – 1 November 2003.

[3] Shayan, A and Morris, H (2005): Combined deterioration problems in a coastal bridge in NSW, Australia. Asian Journal of Civil Engineering (Building & Housing), Vol. 6, No. 6: 477-493.

[4] Famy, C (1999): Expansion of heat-cured mortars. Ph.D Thesis, submitted to the Imperial College, University of London: 256 pp.

[5] Erlin, B (Editor), (1999): Ettringite: the sometimes host of destruction, ACI SP-177, ACI Farmington Hills, Michigan, USA: 261pp.

[6] Scrivener, K. and Skalny, J. (Editors), (2002): Internal sulfate attack and delayed ettringite formation. Rilem Proceedings PRO 35, Proc. of the International Rilem TC 186-ISA workshop, 4-6 September 2002, Villars, Switzerland: 297pp.

[7] Shayan, A., Xu, A. and Tagnit-Hamou, A. (2004): Effects of cement composition and temperature of curing on AAR and DEF expansion in steam-cured concrete. In: Proc.12th International AAR Conference, Beijing, China, October 2004: 773-788.

[8] Wigum, B.J. and Thorenfeldt, E. (2004): Sheets of carbon fibre reinforced polymers (CFRP) as a repair material in order to strengthen and repair concrete damaged by alkali-aggregate reaction. In: Proc.12th International AAR Conference, Beijing, China, October 2004: 1289-1298.

[9] Shayan, A., Xu, A. and Hii, A. (2006): Causes of deterioration of precast bridge piles: An experimental study. Proc. 6th Austroads Bridge Conference, Perth, Western Australia, Sept 2006, 14pp.

TABLE 1: Variables used for casting of experimental model piles.

Factor	Variables	Levels
Aggregate reactivity	3	(Hr), (Lr), and (Nr).
Initial Curing	2	Normal curing, 20 °C (N); Steam-curing, 85 °C (S)
cement SO_3 content	2	2.6 % (native SO_3) in piles 1-12, and 5 % (by added gypsum) in piles 13-16 to induce DEF
Exposure	3	Atmospheric, tap water (W), 3.5% salt water (C)

TABLE 2: Details of strain gauges used.

Strain Gauge type	Gauge length (mm)	Description
CEA-06-250UN-120	6	Steel surface strain gauge
CEA-06-W250A-120	6	Steel weldable strain gauge
N11-FA-60-120-11	60	Concrete surface strain gauge
EGP-5-120	120	Concrete embedded strain gauge
FISO fibre optic	N/A	Steel surface strain gauge
FISO embedded fibre optic	60	Concrete embedded strain gauge

TABLE 3: Strain gauge designation.

TM2W	Top half, Main bar, 2nd bar, Welded strain gauge
TM4S	Top half, Main bar, 4th bar, Surface strain gauge
TS2	Top half, Shear reinforcement, 2nd leg
TS4	Top half, Shear reinforcement, 4th leg
BS4	Bottom half, Shear reinforcement, 4th leg
BM2S	Bottom half, Main bar, 2nd bar, Surface strain gauge
BM4S	Bottom half, Main bar, 4th bar, Surface strain gauge
BS2	Bottom half, Shear reinforcement, 2nd leg
TCC	Top half, Concrete embedded strain gauge, Centre of beam
TCS	Top half, Concrete embedded strain gauge, Side of beam
BCC	Bottom half, Concrete embedded strain gauge, Centre of beam
BCS	Bottom half, Concrete embedded strain gauge, Side of beam
TC3	Top half, Concrete surface strain gauge, 3rd surface
TC4	Top half, Concrete surface strain gauge, 4th surface
BC3	Bottom half, Concrete surface strain gauge, 3rd surface
BC4	Bottom half, Concrete surface strain gauge, 4th surface
C#TS	Pile #, Top half, Steel type fibre optic sensor
C#TC	Pile #, Top half, Concrete type fibre optic sensor
C#BS	Pile #, Bottom half, Steel type fibre optic sensor
C#BC	Pile #, Bottom half, Concrete type fibre optic sensor

TABLE 4: Expansion of concrete prisms.

Concrete	1-year Expansion (%)
Nr-N	0.010
Nr-S	0.003
Lr-N	0.032
Lr-S	0.178
Hr-N	0.140
Hr-S	0.166

TABLE 5: Properties of materials used for repair of piles.

CFRP Wrapping		Concrete jacketing	
CFRP type	MBrace CF 130	Concrete type	Non-reactive aggregate < 7mm
Fibre reinforcement	High tensile carbon	Cement content	450 kg/m^3
Fibre density	1.7 g/cm3	28-day strength	40 MPa
Fibre modulus	240GPa	New pile shape	Square concrete section
Fibre weight (CF)	300g/m2	New cross section	400 x 400 mm
Thickness	0.176mm	Reinforcement details of concrete jacket	4Y16 (Longitudinal) R10 Hoop @250 mm spacing staggered with existing hoop
Tensile strength	3800MPa	New reinforcement ratio	1.3%
Tensile elongation	1.55%	Strain gauges in jacket	2 (top and bottom)

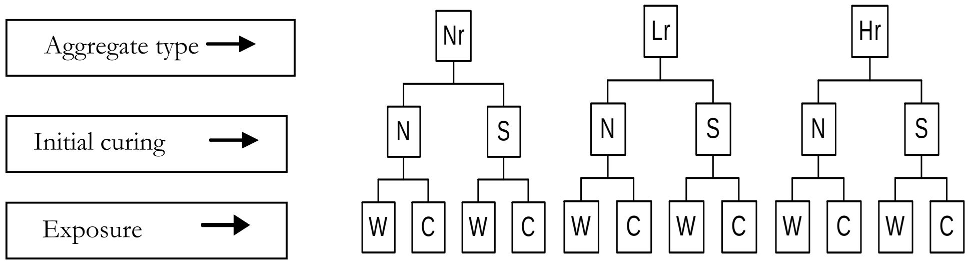

Figure 1a: Combination of variables in the first set of 12 piles (1-12).

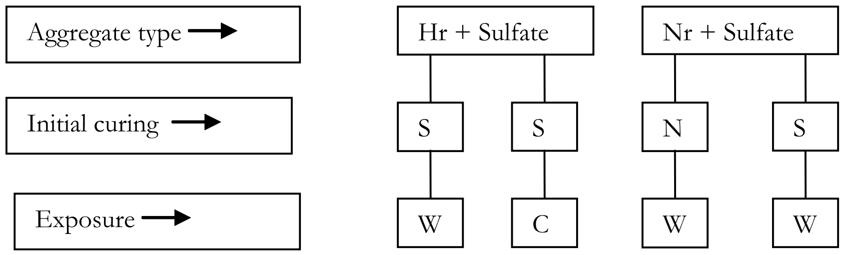

Figure 1b: Combination of variables in the second set of four piles (13-16).

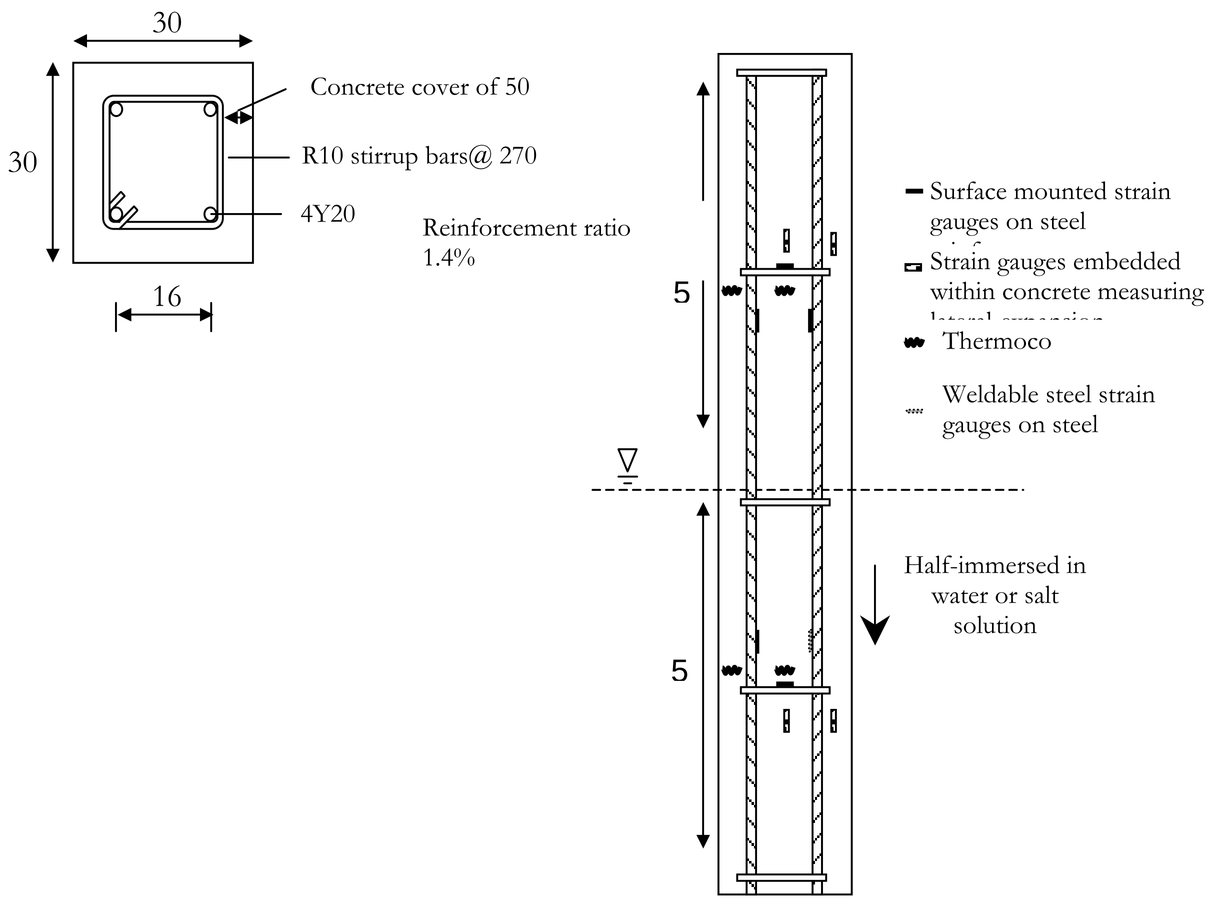

Figure 2: Cross section and reinforcement details of pile specimen.

Figure 3: Steel cage.

Figure 4: Finished pile.

Figure 5: Storage of pile.

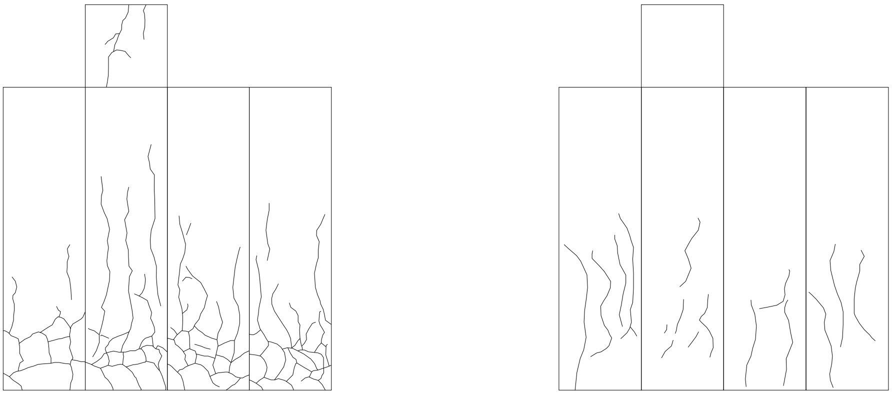

Figure 6: Cracking developed in pile 11 at two years (left) and in pile 14 at one year (right).

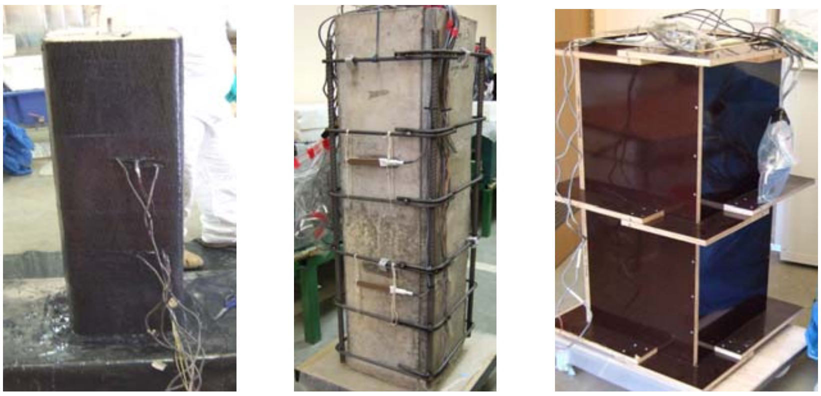

Figure 7: Views of model piles after repair with CFRP (left); fitted with reinforcement (centre) and after fitting mould for casting concrete jacket (right).

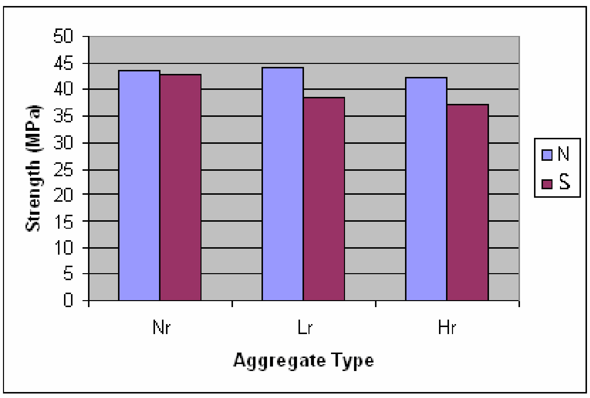

Figure 8: compressive strength at 28 days.

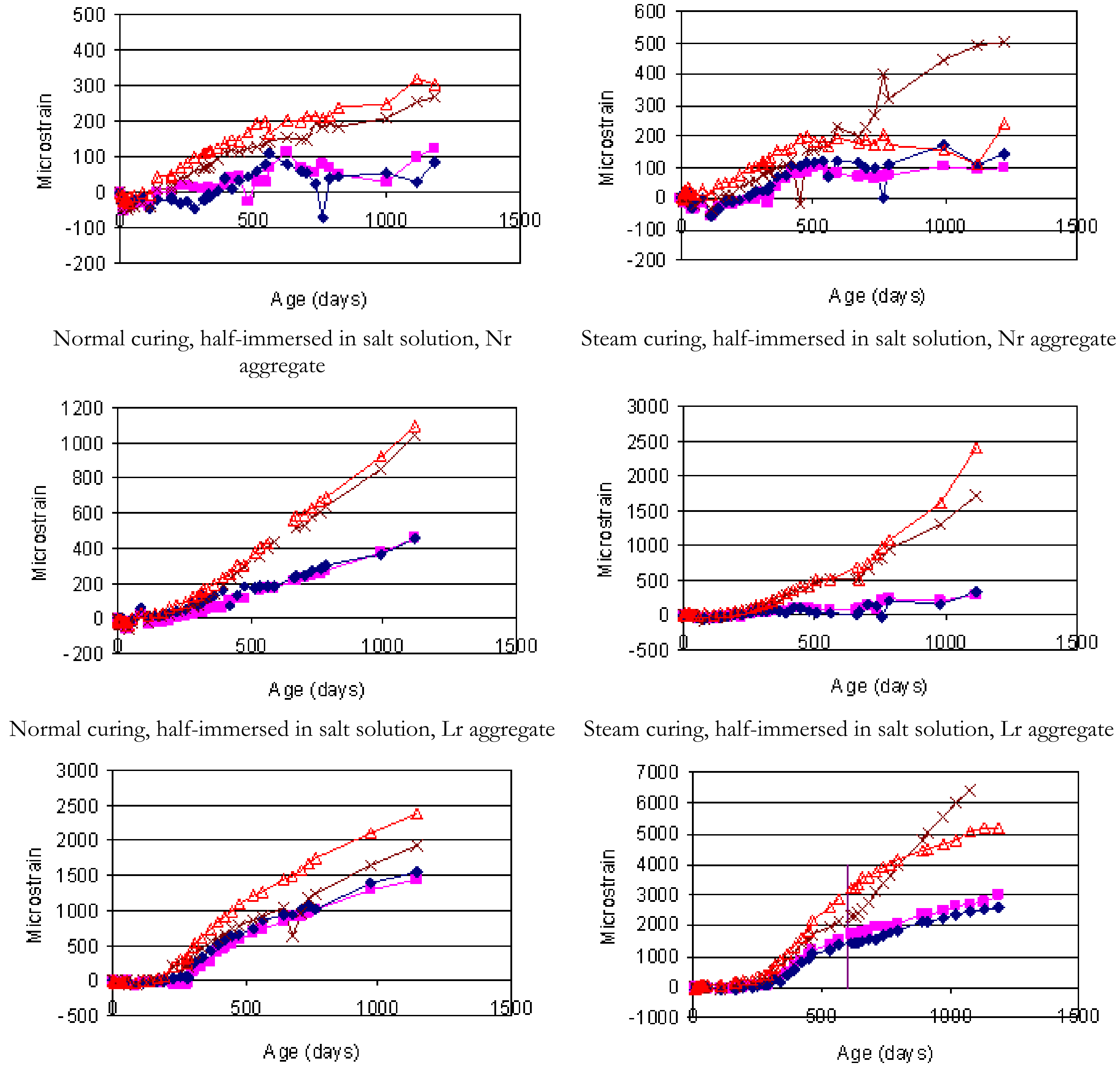

Normal curing, half-immersed in salt solution, Nr aggregate

Steam curing, half-immersed in salt solution, Nr aggregate

Normal curing, half-immersed in salt solution, Lr aggregate

Steam curing, half-immersed in salt solution, Lr aggregate

Normal curing, half-immersed in salt solution, Hr aggregate

Steam curing, half-immersed in salt solution, Hr aggregate

TCS - Concrete gauge on top half and at side of pile
TCC - Concrete gauge on top half and at centre of pile
BCS - Concrete gauge on bottom half and at side of pile
BCC - Concrete gauge on bottom half and at centre of column

Figure 9: Concrete expansion measured by the embedded gauges in piles containing the three different aggregates.

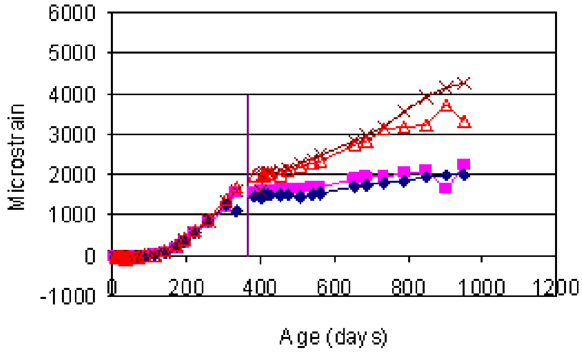

Pile 13- Steam curing, half-immersed in water, Hr aggregate, 5% SO_3

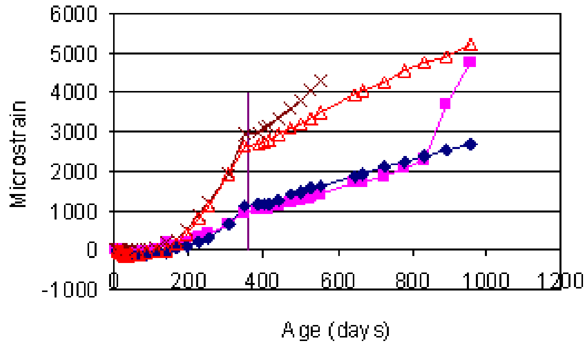

Pile 14- Steam curing, half-immersed in salt solution, Hr aggregate, 5% SO_3

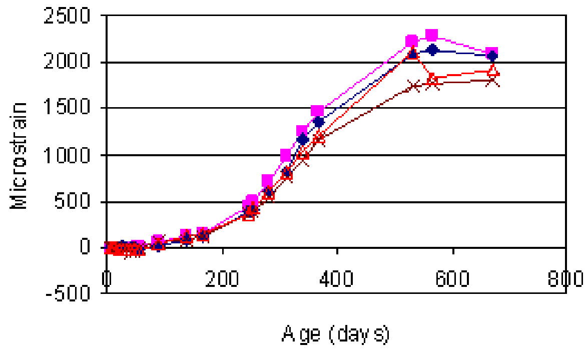

Pile 15- Steam curing, half-immersed in water, Nr aggregate, 5% SO_3

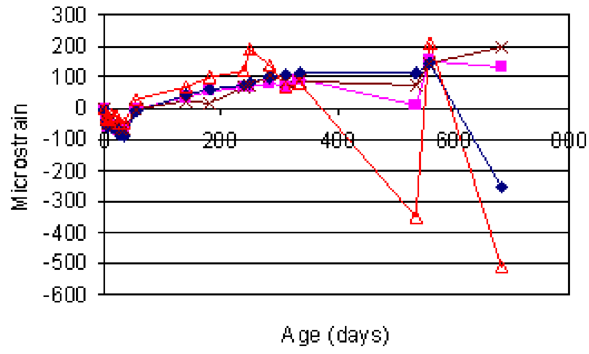

Pile 16- Normal curing, half-immersed in water, Nr aggregate, 5% SO_3

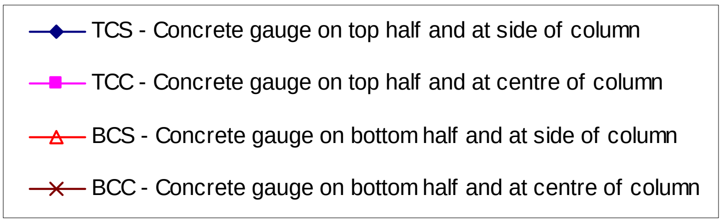

Figure 10: Concrete strain measured by embedded gauges in piles with higher sulfate content.

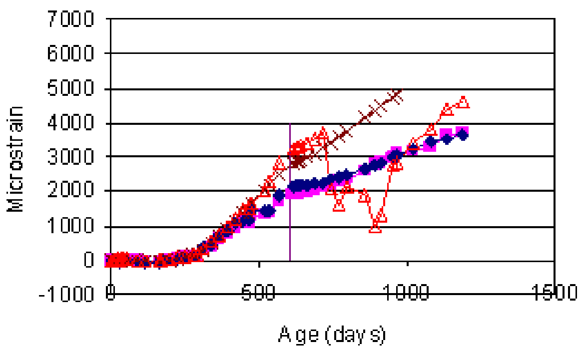

Pile 10- Steam curing, half-immersed in water. Hr aggregate, 2.6% SO_3

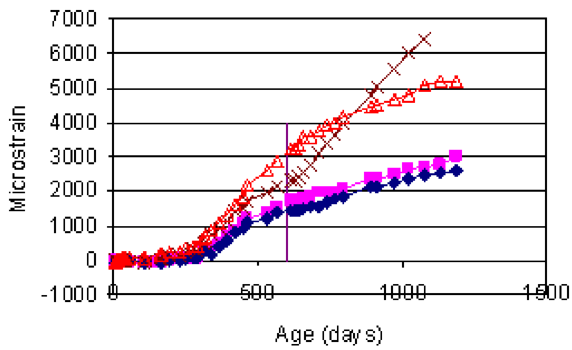

Pile 11- Steam curing, half-immersed in salt solution. Hr aggregate, 2.6% SO_3

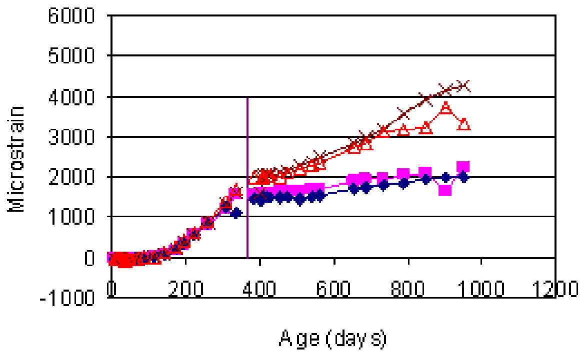

Pile 13- Steam curing, half-immersed in water, Hr aggregate, 5% SO_3

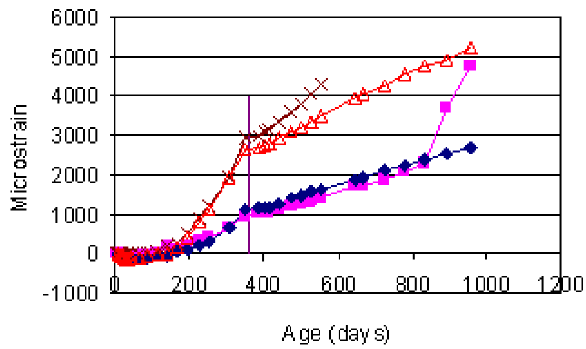

Pile 14- Steam curing, half-immersed in salt solution, Hr aggregate, 5% SO_3

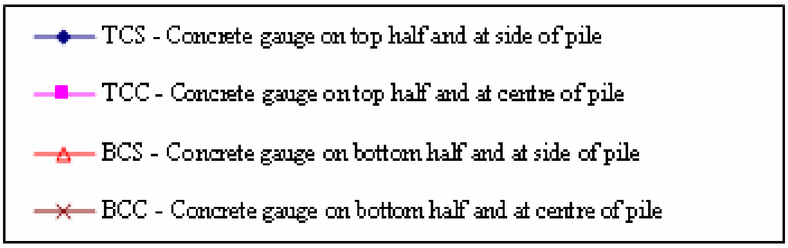

Figure 11: Comparison of concrete expansion in piles containing the reactive aggregate and either 2.6% SO_3 (piles 10 & 11) or 5% SO_3 (Piles 13 &14).

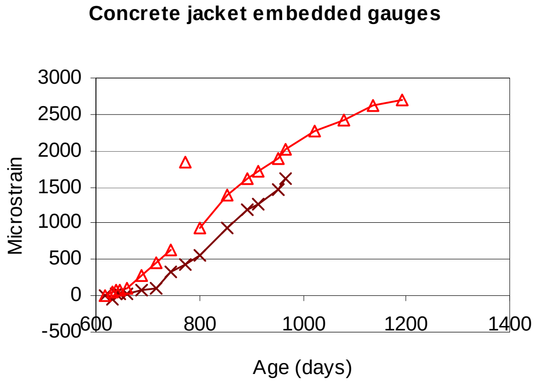

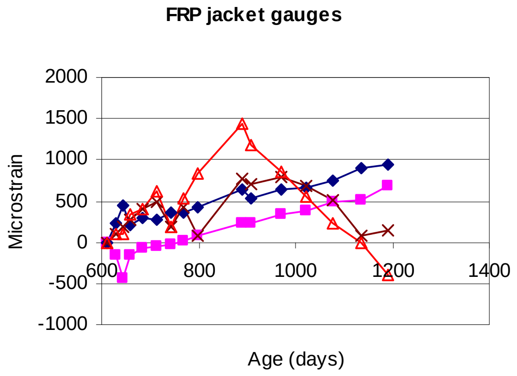

Steam curing, half-immersed in salt solution

Steam curing, half-immersed in water.

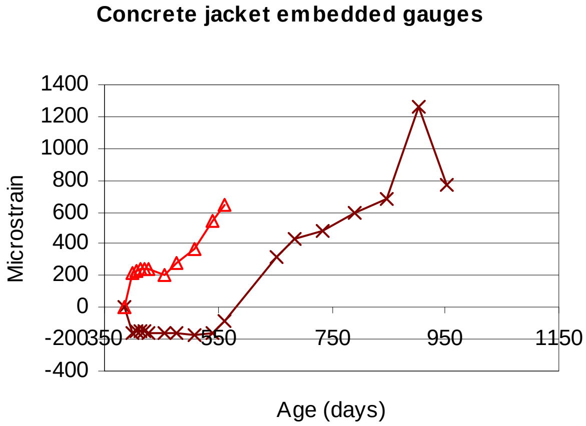

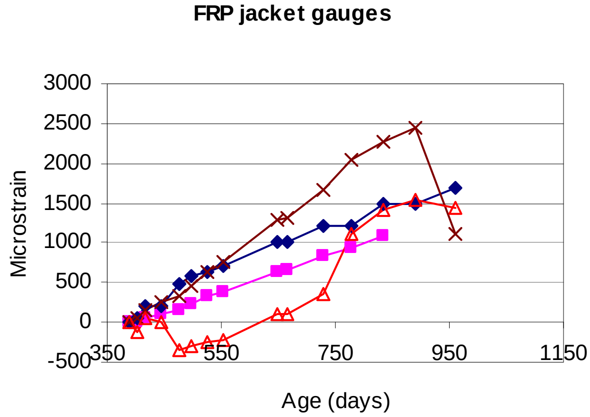

Highly reactive concrete, steam curing, half-immersed in water. Highly reactive aggregate, high sulphate

Highly reactive concrete, steam curing, half-immersed in salt solution. Highly reactive aggregate, high sulphate.

Concrete jacket embedded gauges

- TCSN-Top half, Concrete embedded strain gauge, Concrete Jacket
- BCSN-Bottom half, Concrete embedded strain gauge, Concrete Jacket

FRP jacket embedded gauges

- TF4S-Top half, FRP, 4th side, surface strain gauge
- TF2S-Top half, FRP, 2nd side, surface strain gauge
- BF4S-Bottom half, FRP, 4th side, surface strain gauge
- BF2S-Bottom half, FRP, 4th side, surface strain gauge

Figure 12: Strain developments in jackets of columns with highly reactive aggregate (Columns 10-11, and 13-14).

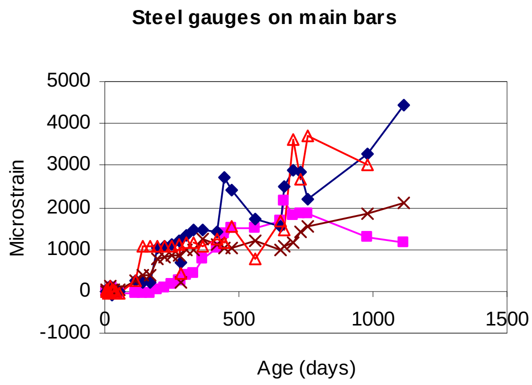

Normal curing, half-immersed in water

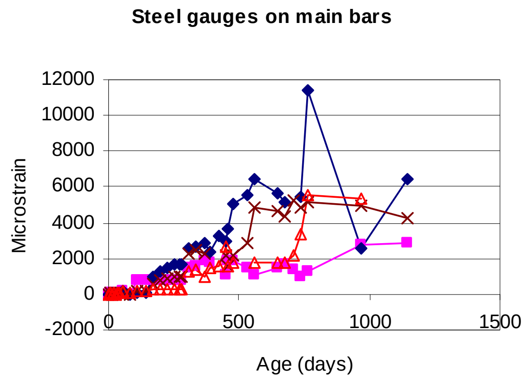

Normal curing, half-immersed in salt solution

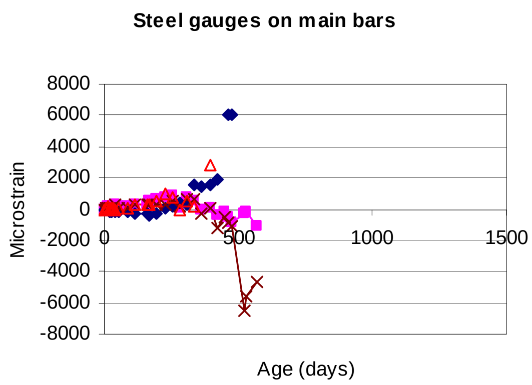

Steam curing, half-immersed in water.

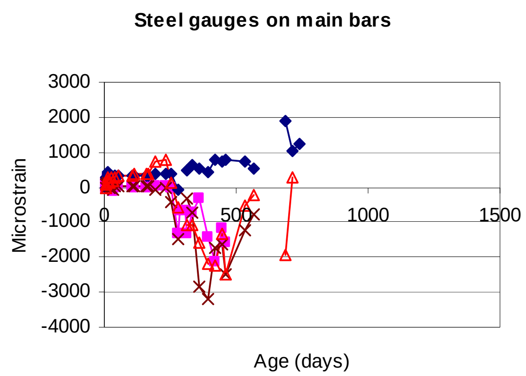

Steam curing, half-immersed in salt solution.

TM2W – Welded gauge on main bar, top half and 2nd side of pile
TM4S – Surface gauge on main bar, top half and 4th side of pile
BM2S – Surface gauge on main bar, bottom half and 2nd side of pile
BM4S – Surface gauge on main bar, bottom half and 4th side of pile

Figure 13: Steel strain development in piles with highly reactive aggregate (piles 9, 12, 10, 11).

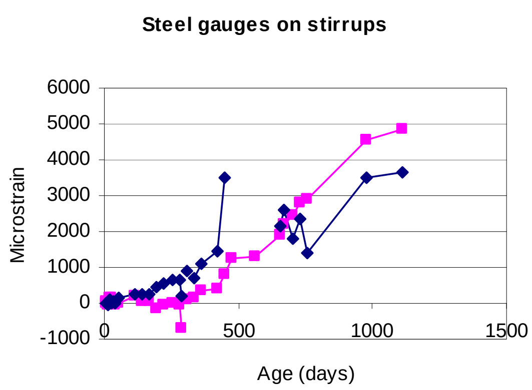

Normal curing, half-immersed in water

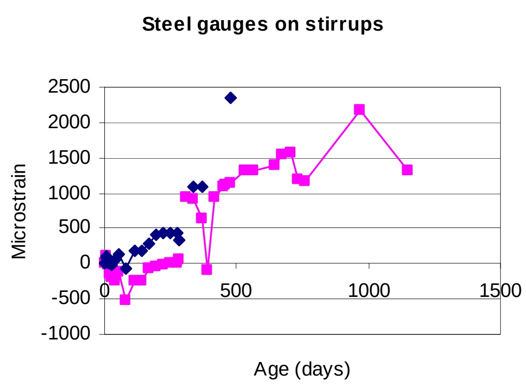

Normal curing, half-immersed in salt solution,

TM2W - Main bar gauge on top half and at 2nd side of pile
TM4S - Main bar gauge on top half and 4th side of pile
BM2S - Main bar gauge on bottom half and 2nd side of pile
BM4S - Main bar gauge on bottom half and 4th side of pile

Figure 14: Strain development in the stirrup of piles made with highly reactive aggregate.

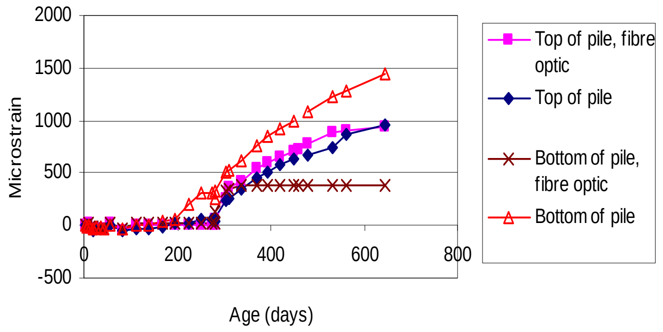

Figure 15: Comparison of readings of fibre optic and foil concrete gauges in Pile 12.

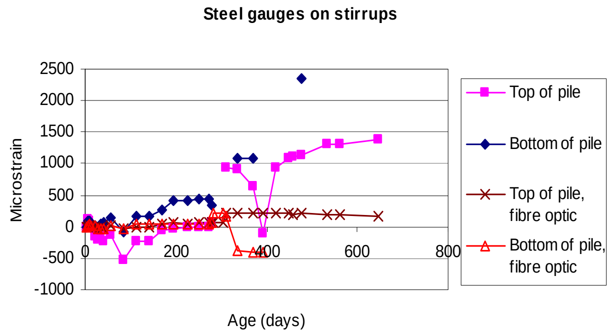

Figure 16: Comparison of readings from the fibre optic and electrical foil gauges installed on steel bars in Pile 12.